Memorias del XVI Congreso Latinoamericano
de Control Automático, CLCA 2014
Octubre 14-17, 2014. Cancún, Quintana Roo, México

Robust Linear Velocity Control of a Car-Like Mobile Robot for Outdoor Applications

Rodolfo Reyes-Báez * **Iván Estrada-Sánchez** **
Martín Velasco-Villa ** **Víctor Cruz-Morales** *
Hugo Rodríguez-Cortés ***,⋆

* *Engineering Division, Autonomous Technological Institute of Mexico (ITAM), Río Hondo 1, Progreso Tizapan, Álvaro Obregón, México, D.F., (e-mail: {rodolfo.reyes, victor.cruz}@itam.mx)*
** *CINVESTAV-IPN, Electrical Engineering Department, Mechatronics Section, Av. IPN, No. 2508, Col. Zacatenco, C.P. 07360, México D.F.,(e-mail: {ivanestrada, velasco}@cinvestav.mx)*
*** *Centro de Desarrollo Aeroespacial del Instituto Politécnico Nacional, Belisario Domínguez 22, Col. Centro, México, D.F. (e-mail: hrodriguez@cinvestav.mx)*

Abstract: This paper proposes a nonlinear control scheme to command the linear velocity of a car-like mobile robot. The controller aims to overcome the problem of partial knowledge of the dynamic model due to the interaction wheels-terrain for outdoor applications. A proportional-derivative feedback term in conjunction with a disturbance estimator based on the immersion and invariance control design technique compose the proposed controller. The task of the disturbance estimator is to generate a signal that asymptotically cancels the effect of the disturbance. Experiments are included to illustrate the performance of the proposed controller.

Keywords: Robust control, intelligent PD-controller, nonlinear observer, inmersion and invariance (I&I), motion control, hierarchical control.

1. INTRODUCTION

In addition to the wide range of civil and military applications of wheeled mobile robots (WMRs), the nonholonomic nature of their kinematic models has attracted the attention of many researchers. Different control techniques have been proposed to solve the trajectory tracking or path following motion control problems for nonholonomic WMRs. However, the majority of the proposed solutions solve such problems at kinematic model level, thus, they rely on accurate low level velocity controllers.

In order to design a low level velocity controller for a WMR, its dynamic model must be available. The dynamic model of this class of robots accounts for the inertia effects as well as for the interaction between the WMR's power plant and the environment through the wheels. Assuming that the WMR behaves as a rigid body, it is possible to easily obtain a model of the inertia effects. However, the interaction with the environment through the wheels is very difficult to model. It depends on, for example, the nature of the terrain, the material of the wheels, the area of contact of the wheel with the terrain and the velocity of the WMR. Hence, the dynamic model of a WMR contains terms that are at the best partially known. This state of affairs brings out the necessity of velocity controllers that require a minimal knowledge of the dynamic model.

Schmid (1995) presents the main results of ten years of research about the interaction between wheel and terrain using three different approaches. The first approach is an analytical method to obtain mathematical models based on physical laws and experiments; the second method relies on practical experience. Finally, the third method develops a model of the interaction wheel-terrain based on the finite element method.

In Iagnemma and Dubowsky (2002), it is described a framework for terrain characterization and identification, composed of 1) vision-based classification of upcoming terrain, 2) terrain parameter identification via wheel-terrain interaction analysis, and 3) terrain classification based on wheel-terrain contact signatures.

In Chuy et al. (2009), experimental results show that the power consumption of a ground vehicle is terrain dependent and it is a function of both, the turning radius and the linear velocity of the vehicle. In Yu et al. (2010) dynamic models of skid-steered of wheeled vehicle for general planar motion are developed and experimentally verified. The coefficient of rolling resistance, the coefficient of friction, and the shear deformation modulus, which have terrain-dependent values characterize the developed models.

⋆ On sabbatical leave from CINVESTAV-IPN, Electrical Engineering Department, Mechatronics Section, México, D.F.

Despite the complexities on modeling the interaction wheel-terrain, linear velocity controllers have been proposed for dynamic models of WMR. In DeSantis (1995) a dynamic model for a double steering car-like WMR is introduced. The model considers the lateral forces exerted by the tires to be a function of the wheels's side-slip angles. The model is used to design a path-tracking controller that is applicable to car-like WMRs with front-wheel steering as well as to robots with front and rear-wheel steering. In Egerstedt et al. (1998), it is presented the so called *single-track dynamical model* for car-like WMR (see Ackermann et al. (1993)), which is based on the description of balanced forces action on the vehicle longitudinal and lateral directions of the vehicle, and on the torque conditions.

In Stotsky et al. (1999), it is proposed a sliding modes global trajectory tracking algorithm within the single-track dynamical model framework; the algorithm uses measurements of the position, orientation and the yaw rate of the vehicle under unknown vehicle parameters. In Panfilov and Tkachev (2003), a generalization of the single-track dynamical model with side-split effect for the car-like WMR is proposed to design a nonlinear control algorithm which solves the reference tracking problem.

In De Luca et al. (2001) and Low (2012) a two-level control architecture for a differential WMR is presented. The hight-level control is used for motion planning and is based on the kinematic model; low-level control layer is in charge of the execution of high-level control velocity commands under ideal conditions of the terrain.

Bascetta et al. (2009) give a first step towards the design and development of the control of an all-terrain WMR. The description of the lowest layer of the control architecture is presented, i.e., the steering and the throttle control systems together with the choice of the control laws.

In this paper, a nonlinear control scheme for the linear velocity for a car-like WMR is proposed without full knowledge of the dynamic model for outdoor applications. The controller is composed of a proportional feedback term in conjunction with a disturbance estimator based on the immersion and invariance control design technique. The task of the disturbance estimator is to generate a signal that asymptotically cancels the effect of the disturbance in real time. Experiments are included to illustrate the performance of the proposed controller.

The structure of the rest of this note is as follows. Section 2 presents the dynamic model of the car-like WMR and states the control problem. Section 3 introduces the proposed controller as well as the disturbance estimator. Section 4 presents an experimental evaluation of the proposed controller. Finally, Section 5 wraps up this note with some concluding remarks.

2. DYNAMIC MODEL FOR CONTROL

Consider the single steering car-like WMR of Figure 2, with configuration vector of generalized coordinates $q_c = [x \quad y \quad \psi \quad \zeta]^T$ with (x, y) is the Cartesian position, ψ represents the orientation and ζ is the front wheels steering angle. The vector q_c takes values in the configuration space $\mathcal{Q} = \mathbb{R}^2 \times S^1 \times S^1$ and S^1 is the unit circle. Other robot's parameters are described in Table 1.

Table 1. System parameters description

Parameter	Description
η	Instantaneous rotation center angle
CM	Center of mass
$m = 4.5\ kg$	Vehicle's mass
$b = 0.18\ m$	Distance from rear axle to center of mass
$\ell = 0.375\ m$	Distance from rear axle to front axle
$J = 0.17\ kg\ m^2$	Yaw moment of inertia respect to CM

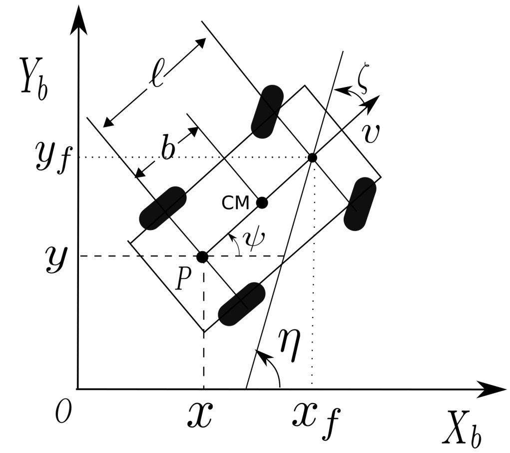

Fig. 1. Car-like mobile robot configuration.

The car-like WMR is a mechanical system with nonholonomic constrains due to assumptions of non-slipping and pure rolling conditions of the wheels (see Bloch (2003) for more details), i.e., they have nonintegrable kinematic constrains of the form

$$A(q)^\top \dot{q} = 0 \tag{1}$$

where $\dot{q}$ is the time derivative of q and $A : \mathcal{Q} \to \mathbb{R}^{n\times m}$ is the nonholonomic constrains matrix function. The general kinematic model for WMRs is given as

$$\dot{q} = G(q)V \tag{2}$$

with V the velocity input which takes values in the tangent space $T_q\mathcal{Q}$ of the configuration manifold at q, and $G : \mathcal{Q} \to \mathbb{R}^{n\times m}$ is a matrix function where their columns form a base of the null space of the nonholonomic constrains matrix function. For the car-like WMR, the kinematic model is

$$\underbrace{\begin{bmatrix} \dot{x} \\ \dot{y} \\ \dot{\psi} \\ \dot{\zeta} \end{bmatrix}}_{\dot{q}_c} = \underbrace{\begin{bmatrix} v\cos(\psi) & 0 \\ v\sin(\psi) & 0 \\ \dfrac{1}{\ell}\tan(\zeta) & 0 \\ 0 & 1 \end{bmatrix}}_{G_c(q_c)} \underbrace{\begin{bmatrix} v \\ F_s \end{bmatrix}}_{V_c}. \tag{3}$$

where v is the linear velocity and F_s the angular velocity of the steering angle ζ.

In motion control problems is a common practice to use hierarchical low-level control schemes that solves the velocity tracking problem for v, then $V_c = [v \quad F_s]^\top$ can be understood as a control input vector. Under the above condition, the dynamic model of the WMR can be seen as a dynamic extension of the kinematic model (2). However, the low-level control is designed under ideal conditions where friction and lateral and slipping forces are not considered.

To overcome the problem of velocity control for outdoor applications, it is necessary to consider at least, the dynamic effects due to lateral and slipping forces. Thus, the dynamical model of the car-like WMR with single steering is given by the folow set of differential equations (DeSantis (1995))

$$\dot{q}_c = G_c(q_c)V_c \tag{4a}$$

$$\dot{v} = g_p F_p(t) - g_u F_u - g_s F_s - g_p \phi(v) \tag{4b}$$

$$J\dot{\Omega} = F_u \ell \sin(\zeta) + F_w \ell \cos(\zeta) \tag{4c}$$

where F_u is the lateral force, F_w is the longitudinal force, F_s the steering command, F_p the traction force and $\phi(v)$ is the tire/road friction force. Function Ω and coefficients g_u, g_p and g_s are defined as follows:

$$\Omega = \frac{v}{\ell}\tan(\zeta) \tag{5a}$$

$$g_p = \left\{ m + \left(\frac{\tan(\zeta)}{\ell}\right)^2 (mb^2 + J) \right\}^{-1} \tag{5b}$$

$$g_u = g_p \left(\frac{1}{\cos(\zeta)}\right) \tag{5c}$$

$$g_s = -\frac{(mb^2 + J)\Omega}{\ell \cos^2(\zeta)} g_p. \tag{5d}$$

The dynamic model (4) was derived with respect to the center of mass (CM) of the system. However, in this research work, there is a special interest to the longitudinal dynamic model with respect to the middle point between the rear wheels, i.e., when $b = 0$. Then, equation (4b) is replaced by

$$\left[m + J\left(\frac{\tan(\zeta)}{\ell}\right)^2 \right] \dot{v} = F_p - \frac{1}{\cos(\zeta)} F_u + \frac{J\Omega}{\ell\cos^2(\zeta)} F_s - \phi(v). \tag{6}$$

Notice that for real cars, the steering angle is limited by mechanical structure. If $\zeta \in [-\pi/4, \pi/4]$, it is possible to neglect the second sum term of acceleration's coefficient in equation (6). Then we have,

$$m\dot{v} = F_p - \underbrace{\left[\frac{1}{\cos(\zeta)} \left(F_u - \frac{J\Omega}{\ell \cos(\zeta)} F_s \right) + \phi(v) \right]}_{\Phi(v,\zeta)}. \tag{7}$$

The most common tire friction models used in the literature are those described by algebraic slip/force relationships. They are defined as one-to-one maps between the friction $\phi(v)$, and the longitudinal split rate, which is defined as

$$s = \begin{cases} s_b = \dfrac{r\omega}{v} - 1, & \text{if } v > r\omega, v \neq 0 \text{ for breaking} \\ s_d = 1 - \dfrac{v}{r\omega}, & \text{if } v < r\omega, \omega \neq 0 \text{ for driving} \end{cases} \tag{8}$$

with r and ω representing the wheel radius and angular velocity respectively. One of the most well-know models of this type is Pacejka's model (see Pacejka and Sharp (1991) for more details), also known as the "Magic Formula", it has the form

$$\phi(v) = c_1 \sin\left(c_2 \arctan\left\{c_3 s - c_4\left[c_3 s - \arctan(c_3 s)\right]\right\}\right) \tag{9}$$

where the $c_{i=1,\ldots,4}$ parameters can be identified by matching experimental data to characterize this model.

In this work, we assume that the robots is in driving mode, then $s = 1 - \frac{v}{r\omega}$. Due to $v > 0$, it is easy to verify that $\phi(v) > 0$ if $c_2 > 0$. Moreover,

$$||\phi(v)||_\infty = c_1 \sin(c_2). \tag{10}$$

Now, consider the following reduced dynamic model

$$m\dot{v} = F_p - \Phi(v,\zeta). \tag{11}$$

Where we are assuming that $\Phi(v,\zeta) \in \mathcal{L}_\infty$ and there is a constant δ_p such that $|\Phi(v,\zeta)| < \delta_p < \bar{\delta}_p$.

3. CONTROLLER DESIGN

Control objetive: Design a control scheme such that closed loop signals are bounded and system (6) tracks a constant reference of linear velocity v_d.

The control scheme is given by a PD feedback controller in conjunction with a disturbance estimator based on the immersion and invariance (I&I) control design technique (see Astolfi et al. (2008)). Since the disturbance is bounded, we consider a target disturbance behavior,

$$\lim_{t\to\infty} \left[\bar{\delta}_p \tanh\left(\frac{\hat{\delta}_p(t) + \beta(\tilde{v})}{\bar{\delta}_p} \right) \right] = \delta_p \tag{12}$$

where $\delta_p > 0$ is the disturbance upper bound, $\hat{\delta}_p$ and $\beta(\tilde{v})$ are functions to be defined on the estimator design process.

In real automotive vehicles, the traction force is proportional to the throttle magnitude. Therefore, the following parameterization for the traction force is proposed,

$$F_p = P_W \delta_T \tag{13}$$

with $P_W = mg$ the maximal engine traction force parameterized in terms of the weight of the system. $\delta_T \in [0,1]$ is the throttle command.

Substituting the control signal (13) in (11) it is obtained,

$$\dot{v} = g\delta_T - \frac{1}{m}\Phi(v,\zeta). \tag{14}$$

Defining the velocity error as $\tilde{v} := v - v_d$, the error dynamics is,

$$\dot{\tilde{v}} = g\delta_T - \frac{1}{m}\Phi(v,\zeta) - \dot{v}_d \tag{15}$$

Equation (15) is equivalent to,

$$\dot{\tilde{v}} = g\delta_T - \dot{v}_d - \frac{1}{m}\delta_p + \frac{1}{m}\left[\delta_p - \Phi(v,\zeta)\right]. \tag{16}$$

Consider now the following controller,

$$\delta_T = \frac{1}{g}\left[\dot{v}_d - \lambda_p \tilde{v} - \lambda_d \dot{\tilde{v}} + \frac{\bar{\delta}_p}{m} \tanh\left(\frac{\hat{\delta}_p(t) + \beta(\tilde{v})}{\bar{\delta}_p} \right) \right] \tag{17}$$

with λ_p, $\lambda_d > 0$ and $\dot{v}_d$ is the nominal acceleration (zero in this case due to v_d is a constant).

The closed loop error dynamics with the control law (17) produces

$$(1+\lambda_d)\,\dot{\tilde{v}} + \lambda_p \tilde{v} = -\frac{1}{m}\left[\delta_p - \bar{\delta}_p \tanh\left(\frac{\hat{\delta}_p + \beta(\tilde{v})}{\bar{\delta}_p}\right)\right] + \\ + \frac{1}{m}\left[\delta_p - \Phi(v,\zeta)\right]. \quad (18)$$

Consider the disturbance estimation error defined as,

$$z = \delta_p - \bar{\delta}_p \tanh\left(\frac{\hat{\delta}_p + \beta(\tilde{v})}{\bar{\delta}_p}\right). \quad (19)$$

The evolution of z it is obtained now as

$$\begin{aligned}\dot{z} &= -\left[1 - \tanh^2\left(\frac{\hat{\delta}_p + \beta(\tilde{v})}{\bar{\delta}_p}\right)\right]\left[\dot{\hat{\delta}}_p + \frac{\partial\beta(\tilde{v})}{\partial\tilde{v}}\dot{\tilde{v}}\right] \\ &= -\left[1 - \tanh^2\left(\frac{\hat{\delta}_p + \beta(\tilde{v})}{\bar{\delta}_p}\right)\right] \\ &\quad \times\left[\dot{\hat{\delta}}_p + \frac{\partial\beta(\tilde{v})}{\partial\tilde{v}}\left(g\delta_T - \dot{v}_d - \frac{\delta_p}{m} + \frac{\delta_p - \Phi}{m}\right)\right]. \quad (20)\end{aligned}$$

From (19) we have that

$$\delta_p = z + \bar{\delta}_p \tanh\left(\frac{\hat{\delta}_p + \beta(\tilde{v})}{\bar{\delta}_p}\right). \quad (21)$$

Replacing (21) in (20) is obtained,

$$\begin{aligned}\dot{z} &= -\left(1 - \tanh^2\left(\frac{\hat{\delta}_p + \beta(\tilde{v})}{\bar{\delta}_p}\right)\right) \\ &\quad \times\left\{\dot{\hat{\delta}}_p + \frac{\partial\beta(\tilde{v})}{\partial\tilde{v}}\left[g\delta_T - \dot{v}_d - \right.\right. \\ &\quad \left.\left. -\frac{1}{m}\left(z + \bar{\delta}_p \tanh\left(\frac{\hat{\delta}_p + \beta(\tilde{v})}{\bar{\delta}_p}\right)\right) + \frac{\delta_p - \Phi}{m}\right]\right\}.\end{aligned}$$

Defining now,

$$\dot{\hat{\delta}}_p = -\frac{\partial\beta(\tilde{v})}{\partial\tilde{v}}\left[g\delta_T - \dot{v}_d - \frac{1}{m}\bar{\delta}_p \tanh\left(\frac{\hat{\delta}_p + \beta(\tilde{v})}{\bar{\delta}_p}\right)\right]. \quad (22)$$

We have that,

$$\dot{z} = -\left[1 - \tanh^2\left(\frac{\hat{\delta}_p + \beta(\tilde{v})}{\bar{\delta}_p}\right)\right]\frac{\partial\beta(\tilde{v})}{\partial\tilde{v}}\left[-\frac{1}{m}z + \frac{\delta_p - \Phi}{m}\right]. \quad (23)$$

Defining now,

$$\beta(\tilde{v}) = -m\Gamma\tilde{v} \quad \text{and} \quad \frac{\partial\beta(\tilde{v})}{\partial\tilde{v}} = -m\Gamma \quad (24)$$

with $\Gamma > 0$, it is obtained

$$\dot{z} = -\left[1 - \tanh^2\left(\frac{\hat{\delta}_p + \beta(\tilde{v})}{\bar{\delta}_p}\right)\right](z - \delta_p + \Phi). \quad (25)$$

From above developments, the closed loop system with internal loop scheme controller-estimator (17)-(25) is given by

$$(1+\lambda_d)\,\dot{\tilde{v}} = -\lambda_p\tilde{v} - \frac{1}{m}z + \frac{\delta_p - \Phi}{m} \quad (26a)$$

$$\dot{z} = -\left[1 - \tanh^2\left(\frac{\hat{\delta}_p + \beta(\tilde{v})}{\bar{\delta}_p}\right)\right][z - \delta_p + \Phi]. \quad (26b)$$

REMARK *1.* Asymptotic stability of the closed loop system (26) without the disturbance term $-\delta_p + \Phi$ can be established from the Lyapunov function

$$V = \frac{1}{2}\tilde{v}^2 + \frac{1}{2}\sigma z^2$$

with σ a positive constant. Assuming that the disturbance term $-\delta_p + \Phi$ is arbitrarily bounded, practical stability of the closed loop dynamics can be concluded.

4. EXPERIMENTAL RESULTS

In order to experimentally evaluate the proposed controller, it is implemented on an electric car-like prototype from Team Associated. The vehicle is impulsed by a brushless motor for linear motion and a servomotor for the steering, see Figure 2. The car-like is endowed with a Global Positioning System with an inertial measurement unit MTi-G-700, from Xsens, for velocity measurements.

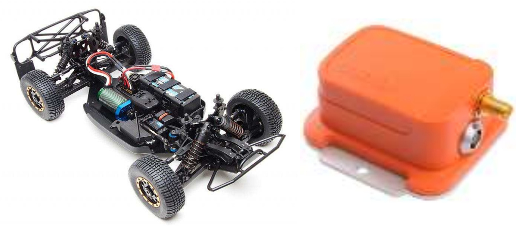

Fig. 2. Car-like WMR and Xsens sensor.

The system is equipped with an embedded system showed in Figure 3. The embedded system consists of several stages. In the first stage, the GPS signals are obtained from a MTi-G Xsens sensor, which are multiplexed and sent to the data storage card and DSP.

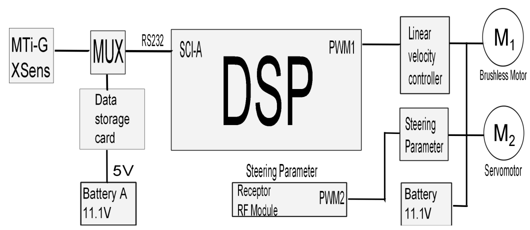

Fig. 3. Functional diagram of the embedded system.

The estimator-controller algorithm runs on the DSP and sends a PWM output signal for the Brushless motor (labeled as PWM1).

For the steering parameter we use a receptor of Radio Frecuency Module (RF) that receives the control signal through a radio-control system, this sends a PWM output signal (PWM2) for the steering servomotor. This allows us to manually control the direction of the WMR.

To evaluate the controller, the experiments were carried out on two different terrains with a reference velocity of $v_d = 2m/s$. The disturbance estimator and controller parameters used for both experiments are shown in Table 2.

Table 2. Estimator and controller parameters.

Parameters	Values
λ_p	1.7
λ_d	1.2
Γ	0.6
δ_p	3.5

The first experiment was carried out on a soccer field, where the disturbance due to the tire/road frictional forces have big influence on the system behavior due to the grass. Fig. 4, shows the behavior of the linear velocity time response. At the beginning of the experiment, about 15 seconds, the WMR is waiting to ensure the availability of the GPS-signals. In this stage, the velocity deviation is about 0.5 m/s due GPS-resolution. The proposed controller achieves the desired reference velocity.

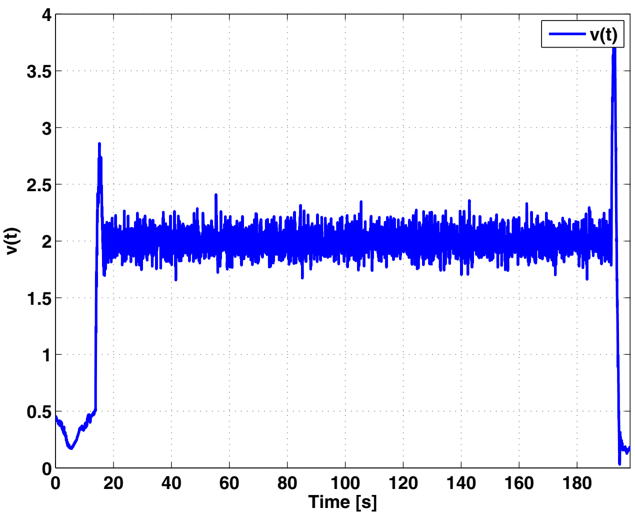

Fig. 4. Linear velocity time response on soccer field.

The velocity at the end of this experiment has an overshoot since the DSP is turned off at this instant and the PWM signal sent to the brushless motor is not controlled. After this phenomena, the DSP does not send output signals anymore.

Fig. 5 shows the path that was taken for the WMR in the $X - Y$ plane. This path was randomly generated by the use of a wireless joystick that manually control the steering wheels.

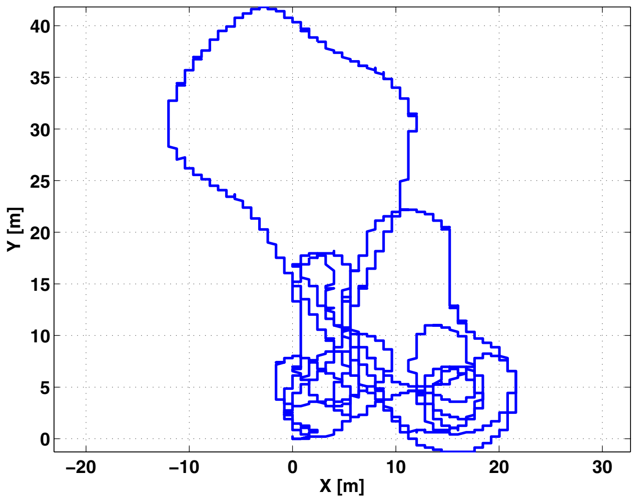

Fig. 5. Path followed for the WMR in the $X - Y$ plane: 1st experiment.

Fig. 6 shows the evolution of velocity error e_v in m/s that remains very close to 0 m/s.

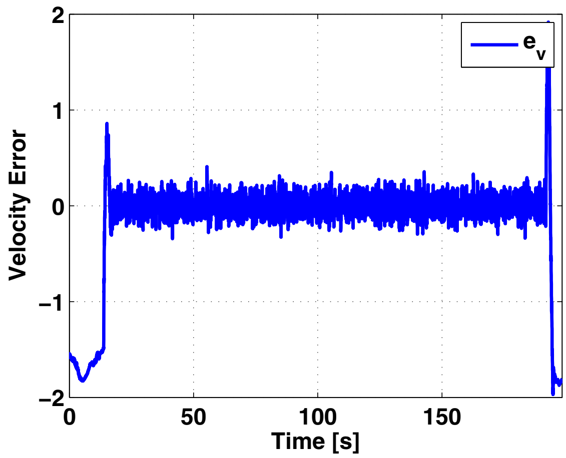

Fig. 6. Velocity error e_v for the first experiment at 2 m/s.

The second experiment was carried out on a flat basketball court. As it can be seen in Fig. 7, the velocity of the WMR is achieved around the desired value.

Fig. 8 shows the path that was taken by the WMR in the $X - Y$ plane for the second experiment.

Finally, Fig. 9 shows the evolution of velocity error e$_v$ in m/s. This velocity error was smaller than the one in the previous experiment.

5. CONCLUSIONS

The regulation problem for linear velocity of a car-like wheeled mobile robot was solved by a robust nonlinear control scheme which consists in proportional-derivative action in conjunction with a disturbance estimator. The estimator was designed using the inmersion and invariance technique. The experiments were carried out in an outdoor environment with the position and velocity measured by a GPS-IMU sensor. The car-like linear velocity converges and remains around the desired reference value. The closed

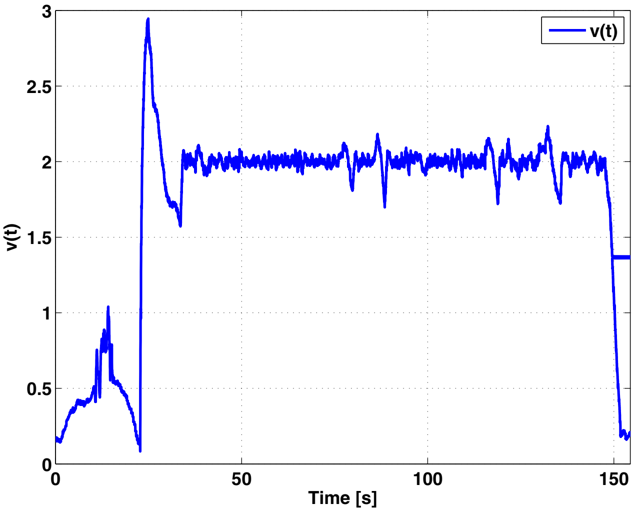

Fig. 7. Linear velocity time response on basketball court.

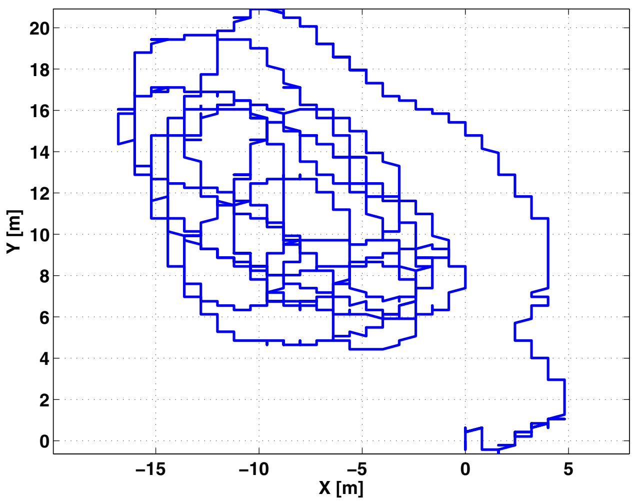

Fig. 8. Path followed for the WMR in the $X - Y$ plane: 2nd experiment.

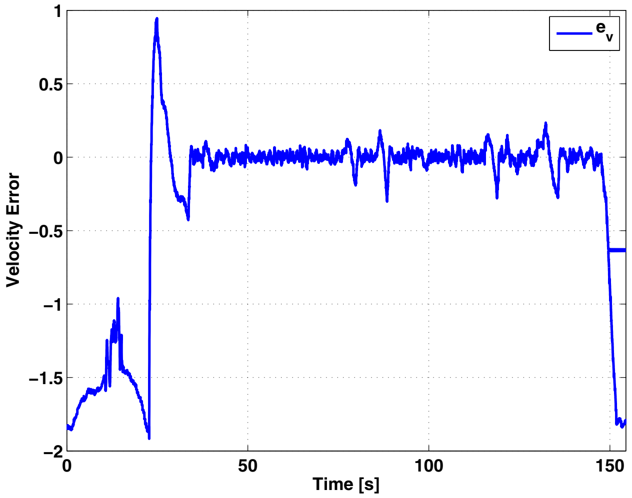

Fig. 9. Velocity error e_v for the second experiment at $2\ m/s$.

loop system performance is acceptable independently of the terrain. The stability proof is not completed because of the nature of the interconnection term $\Phi(v, \zeta)$. Experimental results confirm the theoretical development of the work.

REFERENCES

Ackermann, J., Bartlett, A., Kaesbauer, D., Sienel, W., and Steinhauser, R. (1993). *Robust control*. Springer.

Astolfi, A., Karagiannis, D., and Ortega, R. (2008). *Nonlinear and adaptive control with applications*. Springer Publishing Company, Incorporated.

Bascetta, L., Magnani, G., Rocco, P., and Zanchettin, A.M. (2009). Design and implementation of the low-level control system of an all-terrain mobile robot. In *Advanced Robotics, 2009. ICAR 2009. International Conference on*, 1–6. IEEE.

Bloch, A.M. (2003). *Nonholonomic mechanics and control*, volume 24. Springer.

Chuy, O., Collins Jr, E.G., Yu, W., and Ordonez, C. (2009). Power modeling of a skid steered wheeled robotic ground vehicle. In *Robotics and Automation, 2009. ICRA'09. IEEE International Conference on*, 4118–4123. IEEE.

De Luca, A., Oriolo, G., and Vendittelli, M. (2001). Control of wheeled mobile robots: An experimental overview. In *Ramsete*, 181–226. Springer.

DeSantis, R. (1995). Path-tracking for car-like robots with single and double steering. *Vehicular Technology, IEEE Transactions on*, 44(2), 366–377. doi:10.1109/25.385930.

Egerstedt, M., Hu, X., and Stotsky, A. (1998). Control of a car-like robot using a dynamic model. In *Robotics and Automation, 1998. Proceedings. 1998 IEEE International Conference on*, volume 4, 3273–3278 vol.4. doi:10.1109/ROBOT.1998.680943.

Iagnemma, K.D. and Dubowsky, S. (2002). Terrain estimation for high-speed rough-terrain autonomous vehicle navigation. In *AeroSense 2002*, 256–266. International Society for Optics and Photonics.

Low, C.B. (2012). A trajectory tracking control scheme design for nonholonomic wheeled mobile robots with low-level control systems. In *Decision and Control (CDC), 2012 IEEE 51st Annual Conference on*, 536–543. doi:10.1109/CDC.2012.6426748.

Pacejka, H.B. and Sharp, R.S. (1991). Shear force development by pneumatic tyres in steady state conditions: a review of modelling aspects. *Vehicle system dynamics*, 20(3-4), 121–175.

Panfilov, D.U. and Tkachev, S.B. (2003). Tracking of reference trajectory for wheeled mobile robot. *Process Control*, 3.

Schmid, I.C. (1995). Interaction of vehicle and terrain results from 10 years research at ikk. *Journal of terramechanics*, 32(1), 3–26.

Stotsky, A., Hu, X., and Egerstedt, M. (1999). Sliding mode control of a car-like mobile robot using single-track dynamic model. In *IFAC'99:14th World Congress*. Beijing, China.

Yu, W., Chuy, O.Y., Collins Jr, E.G., and Hollis, P. (2010). Analysis and experimental verification for dynamic modeling of a skid-steered wheeled vehicle. *Robotics, IEEE Transactions on*, 26(2), 340–353.